Turkish National Meeting on Automatic Control
(TOK 2013) , Sept. 25, 2013, Malatya, Turkey

# A Tutorial on Fractional Order Motion Control

Part V: Fractional Order Disturbance Compensations

Prof. YangQuan Chen
Zhuo Li, PhD student
EECS, University of California, Merced
(ychen53, zli32)@ucmerced.edu
**MESA Lab** http://mechatronics.ucmerced.edu

- Fractional Order Motion Controls

John Wiley & Sons, Inc.

Hardcover, 454 pages, December 2012

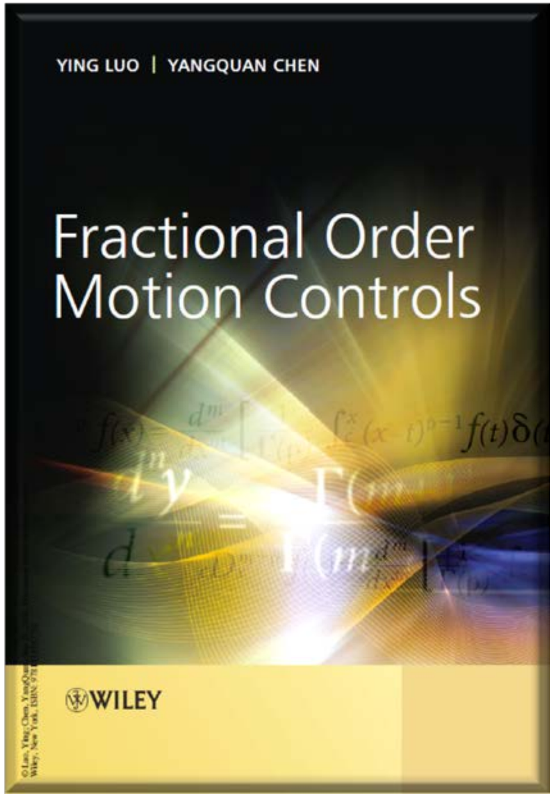



- Dr. Ying Luo

Automation Science and Engineering, South China University of Technology, Guangzhou, PR China

- Dr. YangQuan Chen

Director, Mechatronics, Embedded Systems and Automation (MESA) LAB

MEAM/EECS, School of Engineering,

University of California, Merced

Email: yqchen@ieee.org

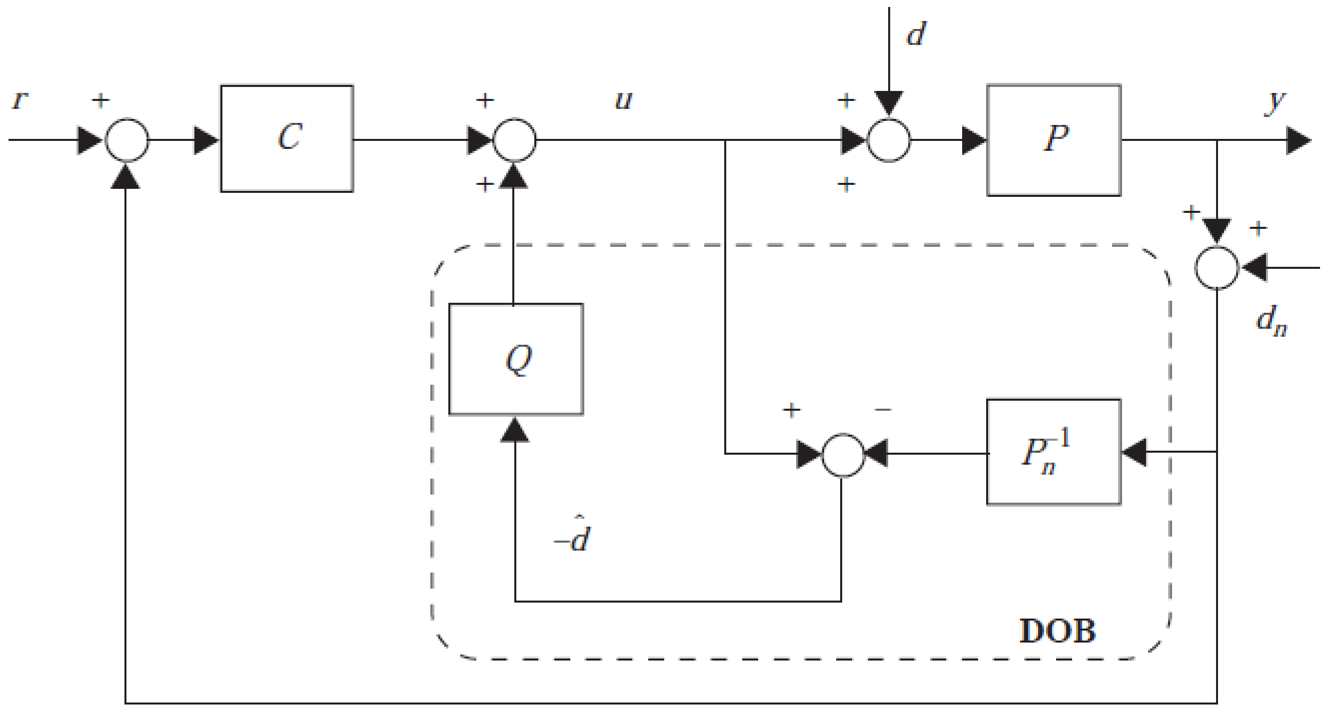


Figure: The conventional disturbance observer block-diagram.

## Design parameters

$n_d$: the number of pure time delays of the control signal
$n_Q$: the relative degree of Q-filter
$\omega_Q$: the cutoff frequency of Q-filter

| The error transfer function | |
|---|---|
| Without DOB | With DOB |
| $S(j\omega) = \dfrac{1}{1 + PC}$ | $S(j\omega) = \dfrac{1}{1 + PC + \delta_{PC}}$<br><br>$\delta_{PC} = \dfrac{P{P_n}^{-1}Q + z^{-n_d}QPC}{1 - z^{-n_d}Q}$ |

## Effects of the design parameters

$n_Q \uparrow \Rightarrow$ phase margin $\downarrow$
$\omega_Q \uparrow \Rightarrow$ phase margin $\downarrow$
A compromise must be made between the disturbance attenuation performance and the robustness of the original system.

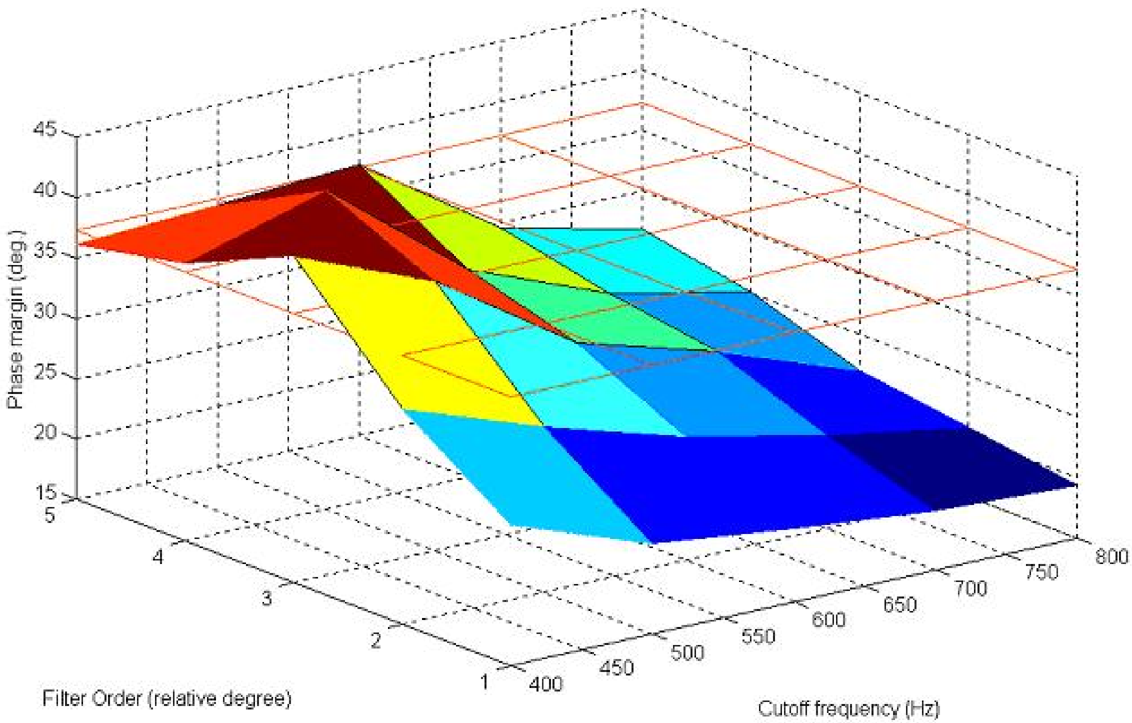


Figure: An illustration of the phase margin (PM) as a function of $n_Q$ and $\omega_Q$ in DOB

## A trade-off solution:

Rule-based switched low pass filtering with varying relative degree
Tuning parameter: $n_Q$

(19) **United States**
(12) **Patent Application Publication**
**Chen et al.**

(10) **Pub. No.: US 2001/0036026 A1**
(43) **Pub. Date: Nov. 1, 2001**

(54) **EFFICIENT SENSORLESS ROTATIONAL VIBRATION AND SHOCK COMPENSATOR FOR HARD DISK DRIVES WITH HIGHER TPI**

(75) Inventors: **YangQuan Chen**, Singapore (SG); **MingZhong Ding**, Singapore (SG); **LeeLing Tan**, Singapore (SG); **KianKeong Ooi**, Singapore (SG)

**Related U.S. Application Data**

(63) Non-provisional of provisional application No. 60/184,718, filed on Feb. 24, 2000.

**Publication Classification**

(51) **Int. Cl.**[7] ........................ **G11B 27/36**; G11B 21/02
(52) **U.S. Cl.** ........................ **360/31**; 360/77.02; 360/75; 360/69

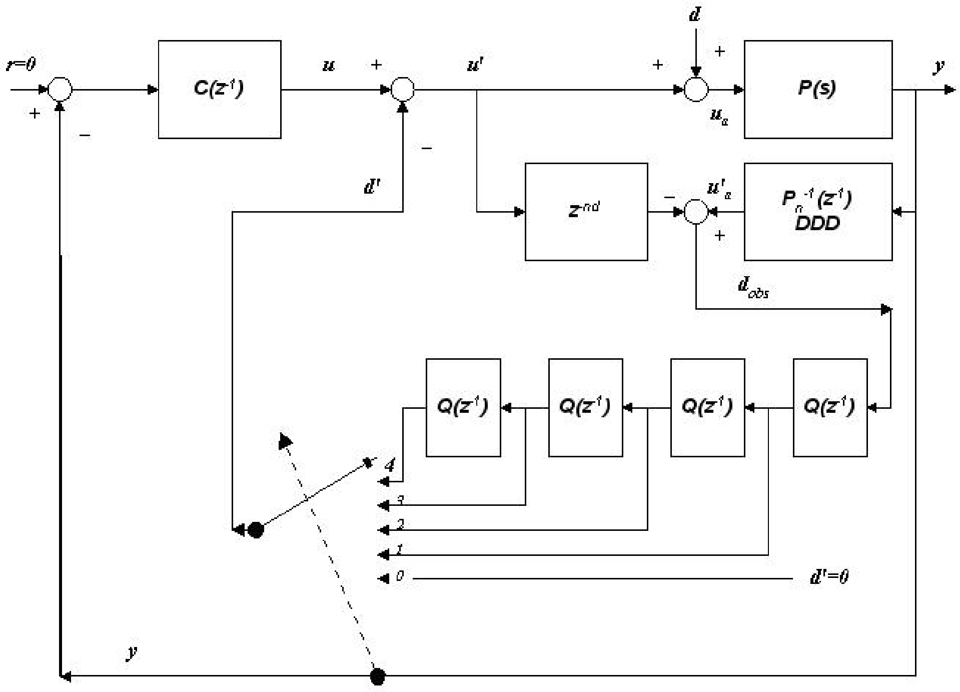


Figure: Q-filter in DOB with a varying relative degree

Figure: A switching policy for the relative degrees of the Q-filter in DOB.

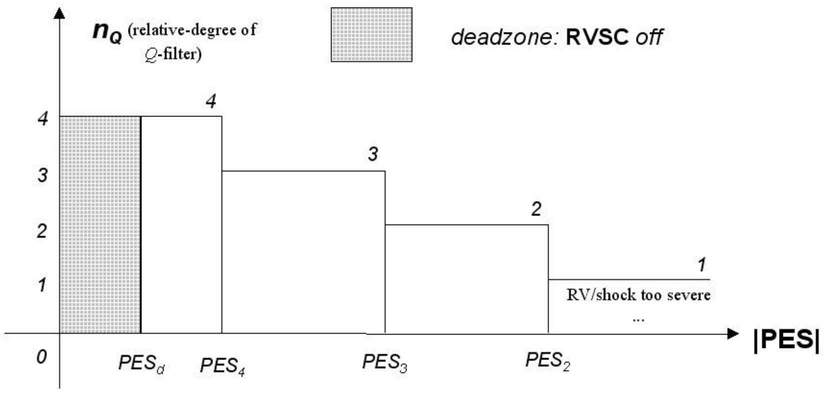

## The proposed trade-off solution:

Fractional order DOB using a fractional order Q filter

$$Q(s) = \frac{1}{(\tau s + 1)^{n_Q}}, \{n_Q | n_Q \in Q, n_Q > 0\}$$

## The implementation

Stable minimum-phase frequency domain fitting

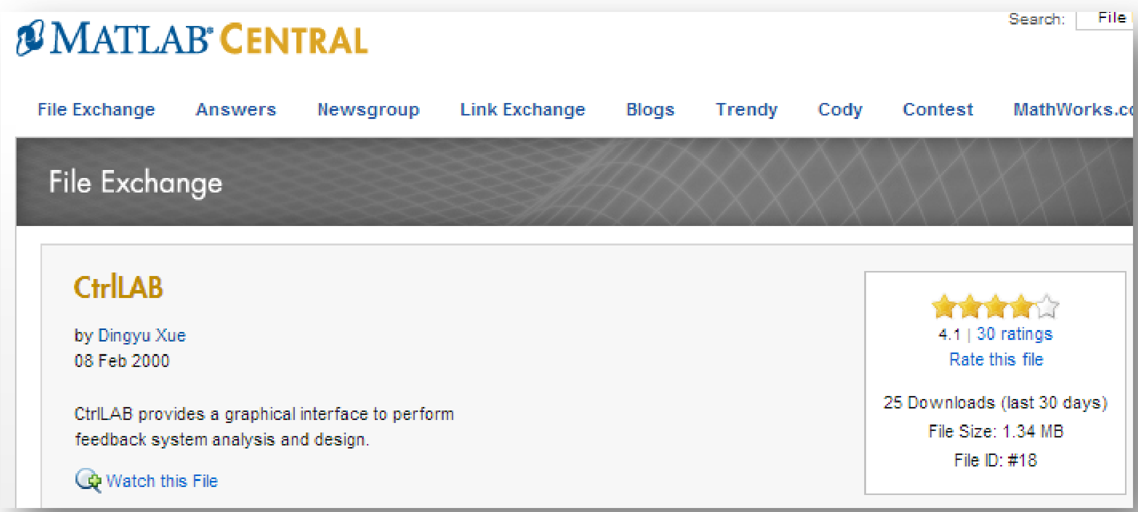

- Periodic disturbance
  - Telecommunication
  - Building vibration

- Periodic disturbance in motion control
  - Repeatable spindle motor runout
  - Cogging force

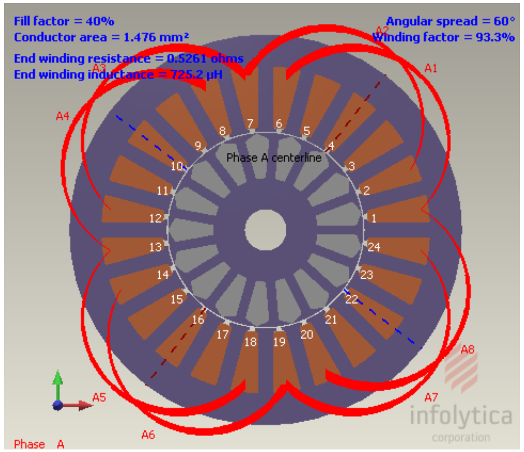


Cogging effect

Tacoma narrow bridge, WA, 1941

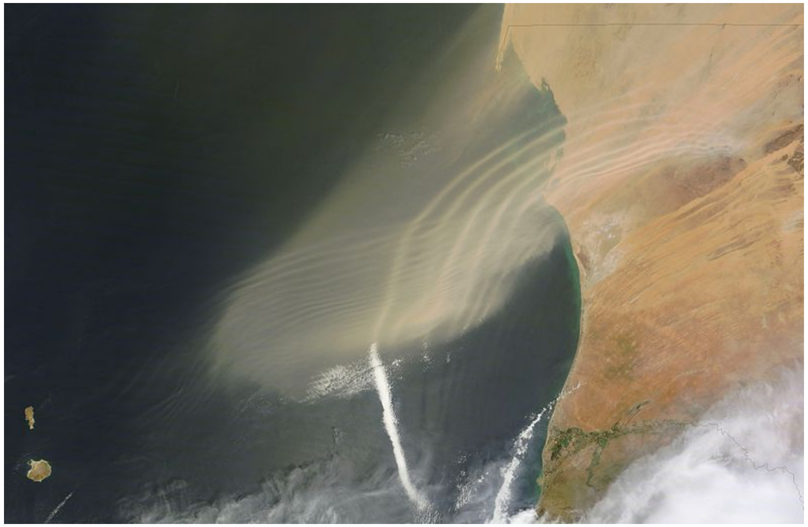

Atmosphere wave
http://en.wikipedia.org/wiki/Atmospheric_wave

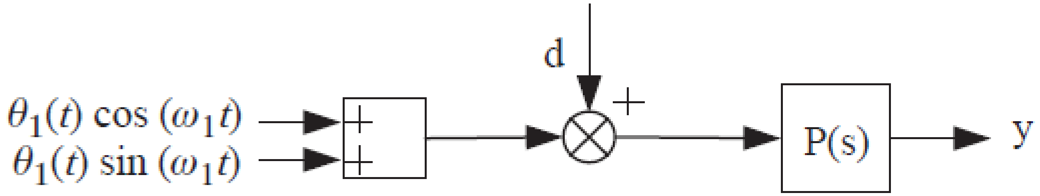


Figure: Fractional order adaptive feed-forward cancellation

## The disturbance

$$d(t) = A\sin(\omega_1 t + \phi) = a_1\cos(\omega_1 t) + b_1\sin(\omega_1 t).$$

## The control input

$$u(t) = \theta_1(t)\cos(\omega_1 t) + \theta_2(t)\sin(\omega_1 t),$$

## The plant output

$$y(t) = Ł^{-1}[Ł((\theta_1(t) - \theta_1^*)\cos(\omega_1 t) + (\theta_2(t) - \theta_2^*)\sin(\omega_1 t))P(s)],$$

## The nominal values

$$\theta_1^* = -a_1, \theta_2^* = -b_1,$$

## The adaptive law

Using Caputo definition for fractional derivative

$${}_0D_t^{\alpha}\theta_1(t) = -gy(t)\cos(\omega_1 t),$$

$${}_0D_t^{\alpha}\theta_2(t) = -gy(t)\sin(\omega_1 t),$$

## The derivation of the adaptive law

$$ {}_0D_t^{\alpha}\theta_1(t) = -\frac{g}{2}y(t)(e^{j\omega_1 t} + e^{-j\omega_1 t}), $$

$$ {}_0D_t^{\alpha}\theta_2(t) = -\frac{jg}{2}y(t)(e^{-j\omega_1 t} - e^{j\omega_1 t}). $$

## The Laplace transform

Using the time shifting property

$$ \Theta_1(s) = -\frac{g}{2s^{\alpha}}(Y(s + j\omega_1) + Y(s - j\omega_1)), $$

$$ \Theta_2(s) = -\frac{jg}{2s^{\alpha}}(Y(s - j\omega_1) - Y(s + j\omega_1)). $$

## The FO adaptive compensator

$$
\begin{aligned}
U(s) = & \frac{1}{2}(\Theta_1(s - j\omega_1) + \Theta_1(s + j\omega_1)) \\
& + \frac{j}{2}(\Theta_2(s - j\omega_1) - \Theta_2(s + j\omega_1)) \\
= & -\frac{g}{2}\left(\frac{1}{(s + j\omega_1)^\alpha} + \frac{1}{(s - j\omega_1)^\alpha}\right) Y(s) \\
= & -gC_{IMP}(s)Y(s),
\end{aligned}
$$

Same !

## The FO internal model principle

$$
C_{IMP}(s) = \frac{(s - j\omega_1)^\alpha + (s + j\omega_1)^\alpha}{2(s^2 + \omega^2)^\alpha}
$$

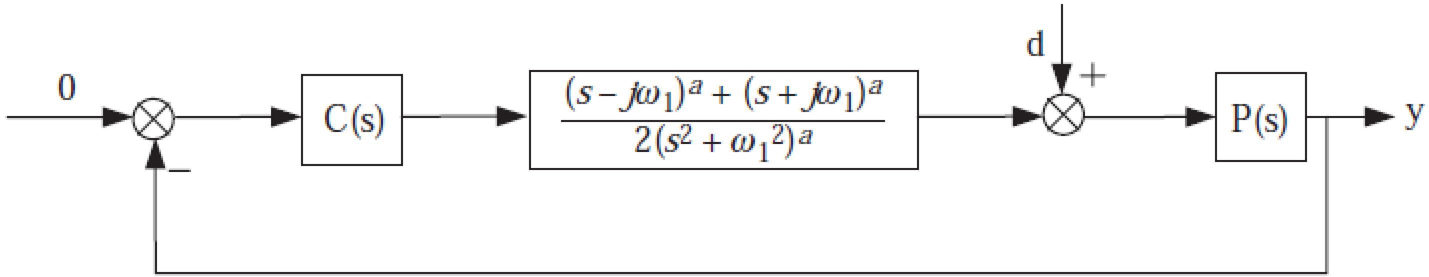


Figure: Fractional order internal model principle equivalence of the fractional order adaptive feed-forward cancellation, with C(s)=g

## The plant and the disturbance

$$P(s) = \frac{s+2}{(s+1)(s+3)},$$

$$d(t) = \sin(0.1t) - 0.2\sin(0.3t),$$

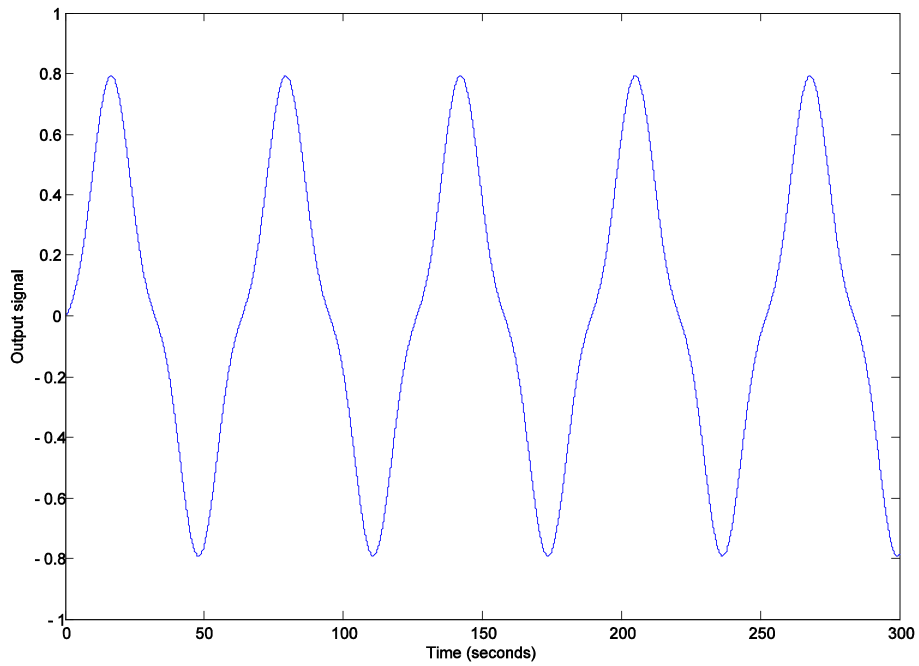


Figure: Plant output without compensation

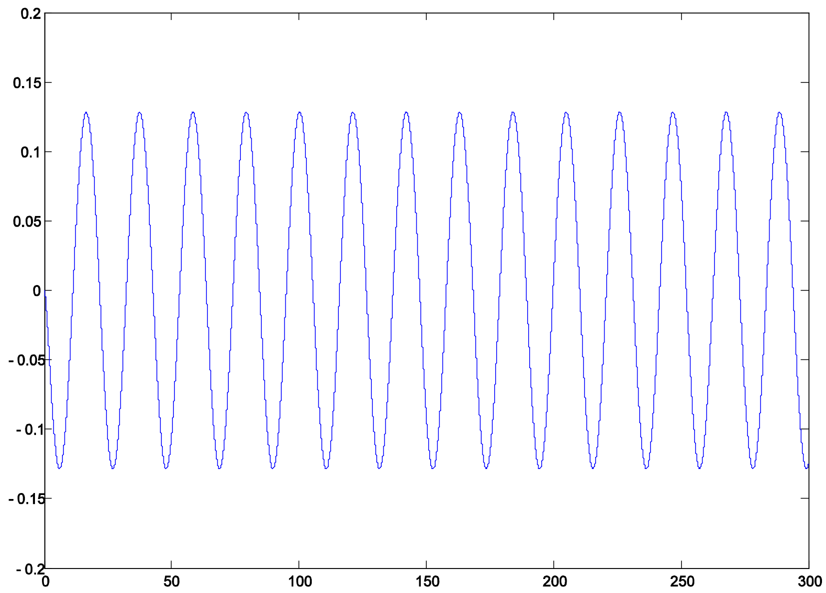


Figure: Plant output with fixed nominal compensation

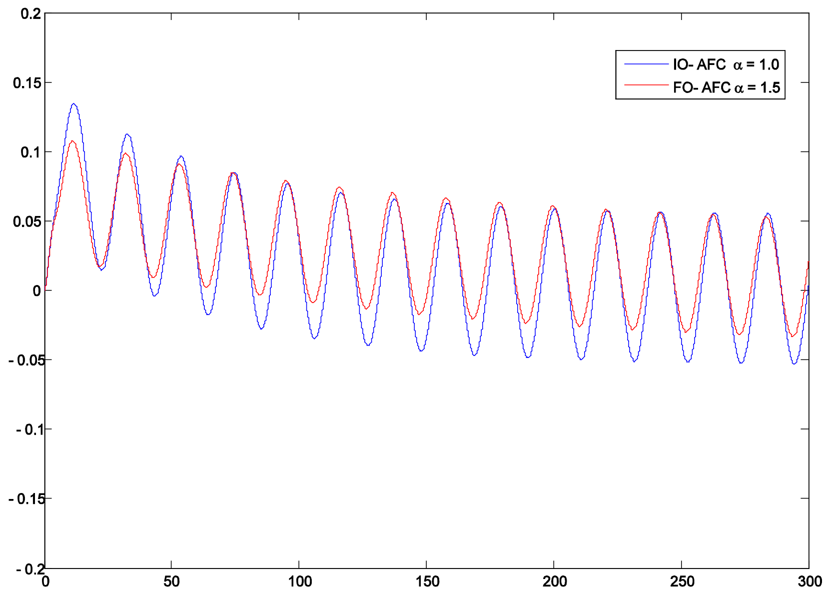


Figure: Plant output with IOAFC compensation and $\alpha = 1.5$ FOAFC

## The sensitivity function

$$G_s(s) = \frac{1}{1 + C(s)C_{IMP}(s)P(s)},$$

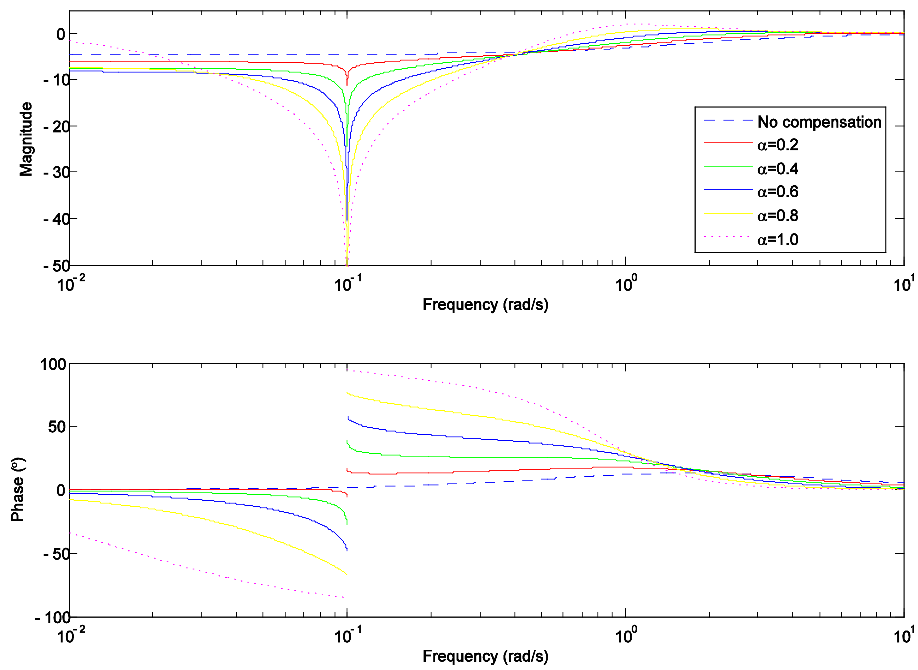


Figure: Bode plots of the sensitivity function with $\omega 1 = 0.1$ and $\alpha \in (0, 1]$

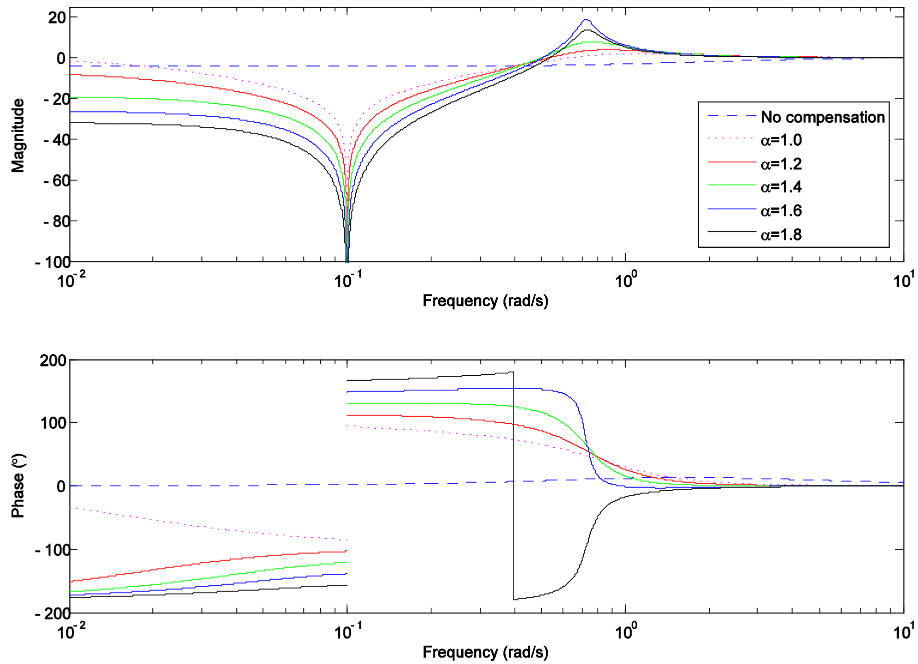


Figure: Bode plots of the sensitivity function with $\omega 1 = 0.1$ and $\alpha \in (1, 2]$

## Comparison

$\alpha \in (0, 1]$, FOAFC is better than IOAFC
$\alpha \in (1, 2)$, IOAFC is better than FOAFC

## The cogging effect

- Trouble maker of PMSM (permanent magnetic synchronous motor)
- Especially at low speed
- Generated by the magnetic attraction between the rotor and the stator
- Appear at $N_{slot-pp} f_s$

## Modeling the cogging force

- Multi-harmonic Fourier expansion

$$F_{cogging} = \sum_{i=1}^{\infty} A_i \, sin(\omega_i x + \varphi_i)$$

- State dependent

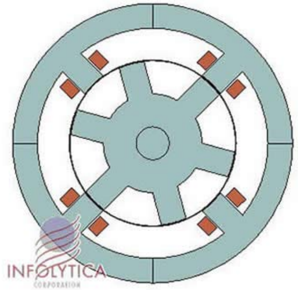

## The plant model

$$\dot{\theta}(t) = v(t),$$
$$\dot{v}(t) = u - \frac{a(\theta)}{J} - T_{l'} - B_1 v,$$
$$u = \frac{1}{J} T_m,\ T_{l'} = \frac{1}{J} T_l,\ B_1 = \frac{B}{J},$$

$\theta$: angular position, $v$: velocity; $a(\theta)$ unknown position-dependent cogging disturbance; $J$: moment of inertia; $T_m$: electromagnetic torque; $T_l$: load torque; $B$: viscous friction coefficient

## The displacement

$$e_\theta(t) = \theta_d(t) - \theta(t)$$
$$e_v(t) = \dot{e}_\theta(t) = v_d(t) - v(t)$$

## The adaptive compensator (AC)

$$u(t) = \dot{v}_d(t) + T_{l'} + \frac{\hat{a}(t)}{J} + \alpha m(t) + \gamma e_v(t),$$

where

$$m(t) := \gamma e_\theta(t) + e_v(t),$$

## The adaptive law for $\hat{a}(t)$

$$\hat{a}(t) = z - \mu v$$

$${}_0D_t^{v} z(t) = \mu[\dot{v}_d(t) + \alpha m(t) + \gamma e_v(t)] + \frac{e_v(t)}{J},$$

$$\begin{cases} v = 1, \mathit{IOAC} \\ v \in (0,1), \mathit{FOAC} \end{cases}$$

## IOAC stability theorem

If the integer order adaptive compensation is used, the equilibrium points $e_\theta$ and $e_v$ are bounded as $t \to \infty$.

## FOAC stability theorem

If the parameters $\alpha, \gamma, and\ \mu$, are chosen to ensure

$$|\arg(\omega_i)| > \lambda \frac{\pi}{2}$$

the equilibrium points $e_\theta$ and $e_v$ are bounded as $t \to \infty$,
Where $\omega_i$ are the roots of

$$w^{2pq+p^2} + aw^{pq+p^2} + bw^{pq} + dw^{p^2} + c = 0,$$

The proof is available in the book

## The applied cogging force

$$F_{cogging} = 2\cos(6\theta) + \cos(12\theta) + 0.5\cos(18\theta)$$

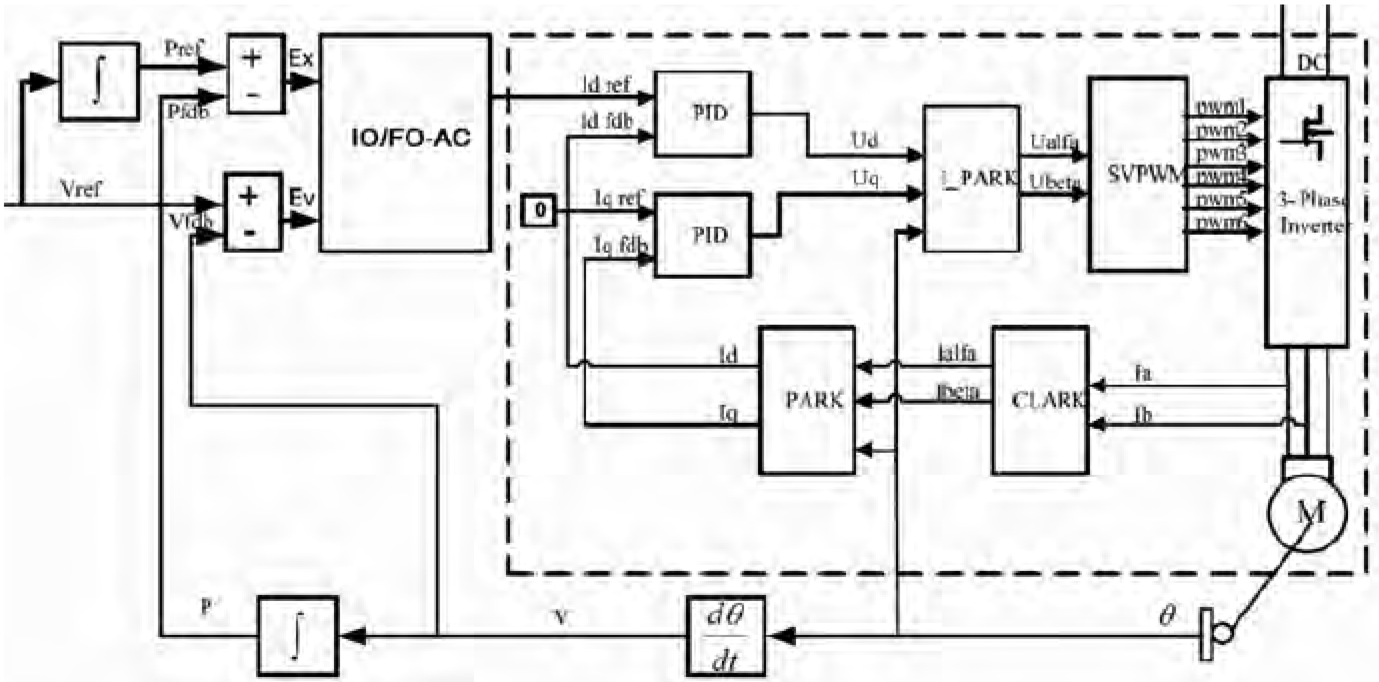


Figure: the block diagram of PMSM servo simulation system with the IO/FOAC for cogging effect compensation

Table: PMSM Specifications

| | | | |
|---|---|---|---|
| Rated power | 1.64 Kw | Rated speed | 2000 rpm |
| Rated torque | 8 Nm | Stator resistance | 2.125 Ω |
| Stator inductance | 11.6 mH | Magnetic flux | 0.387 Wb |
| Number of poles | 6 | Moment of inertia | 0.00289 kgm$^2$ |
| Friction coefficient | 0.0003 Nms | | |

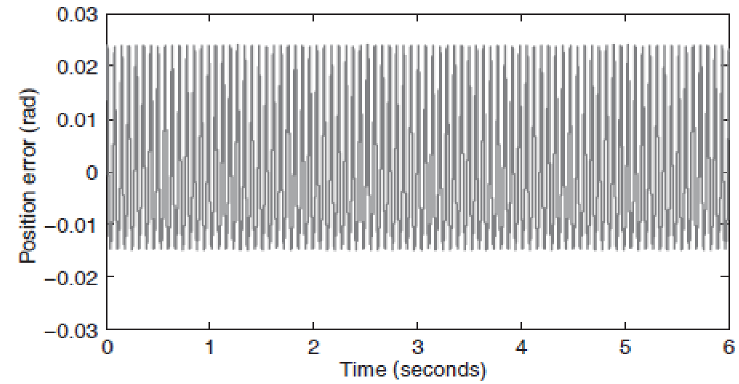


(a) Position

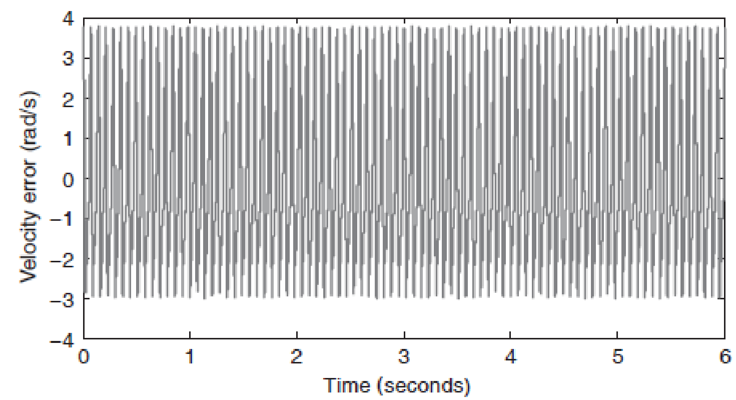


(b) Velocity

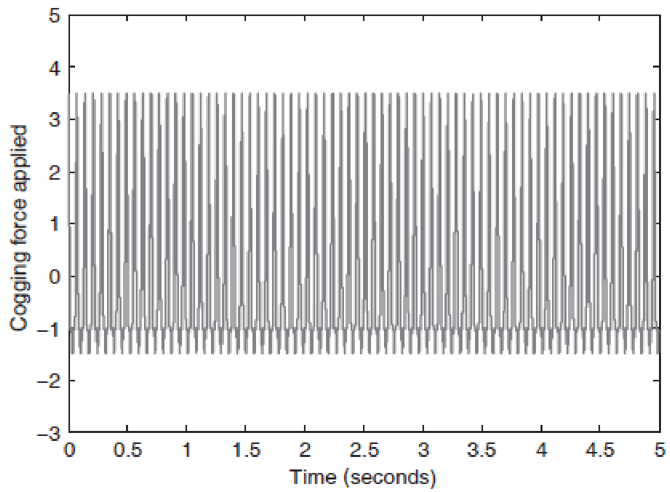


**Figure 15.2** Simulation. Cogging force applied

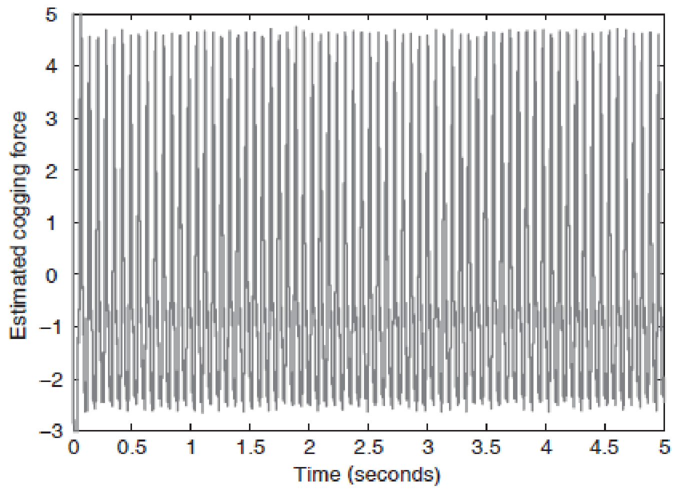


**15.4** Simulation. Estimated cogging force with IOAC ($\nu = 1$)

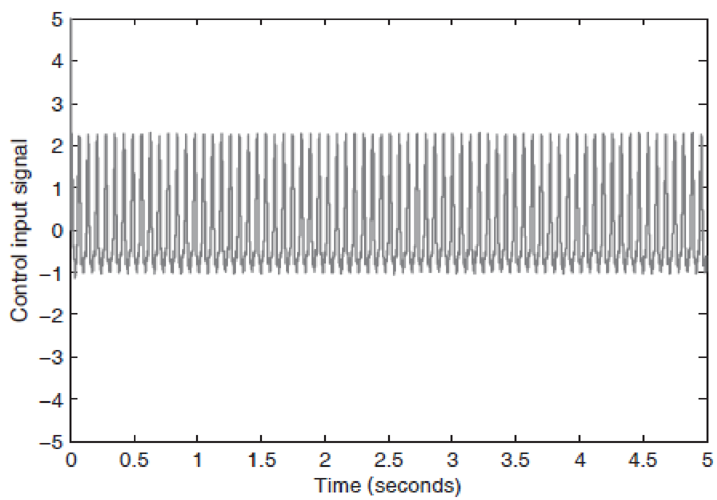


Simulation. Constant reference speed tracking control input signal

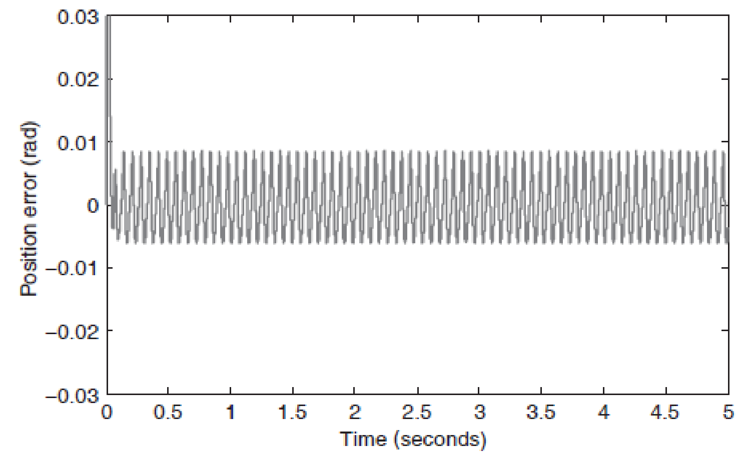


(a) Position

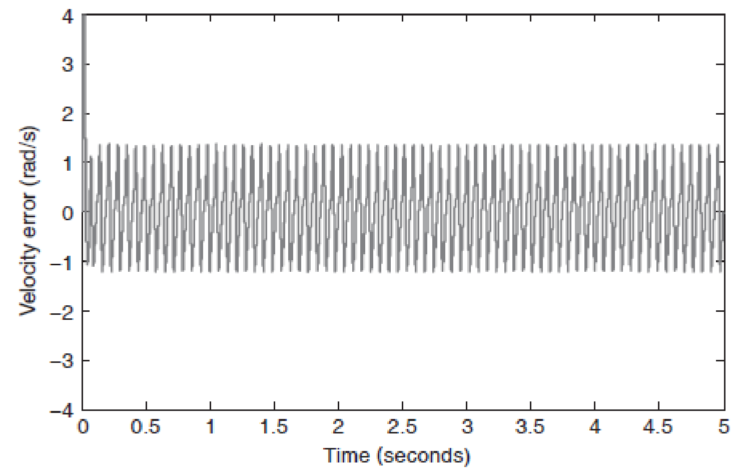


(b) Velocity

Simulation. Constant reference speed tracking errors with IOAC ($\nu = 1$)

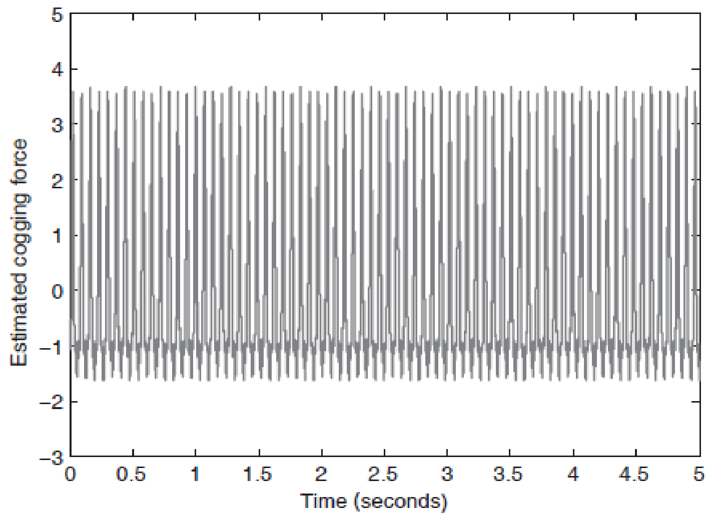


15.7 Simulation. Estimated cogging force with FOAC ($\nu = 0.5$)

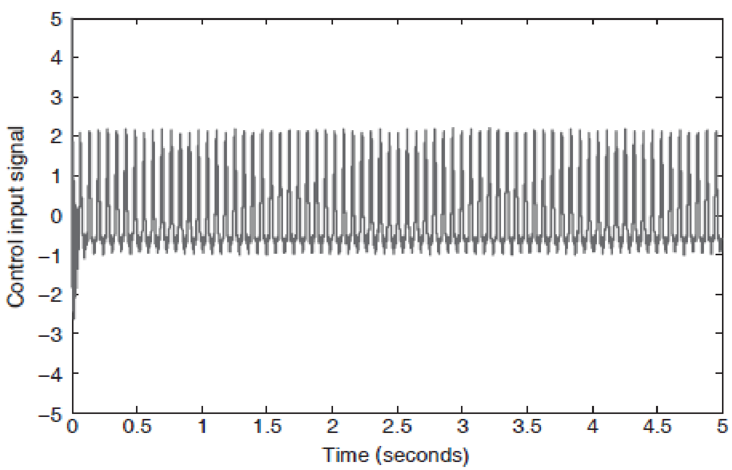


Simulation. Constant reference speed tracking control input signal

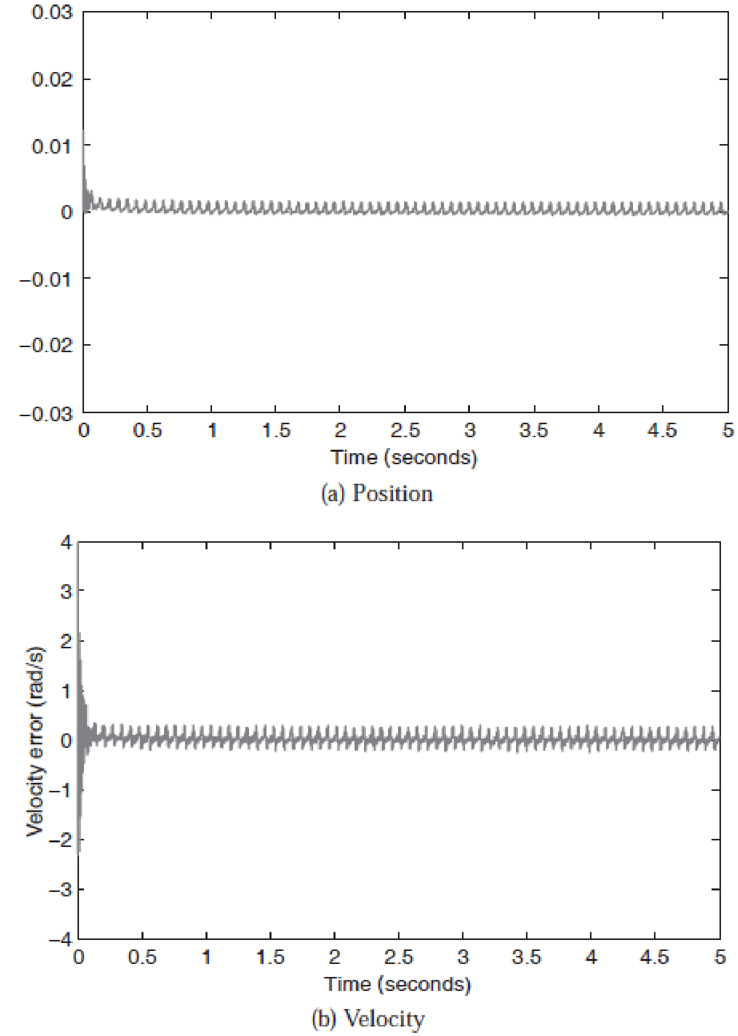


Simulation. Constant reference speed tracking errors with FOAC ($\nu = 0.5$)

## The varying reference speed

$$s_d(t) = \int_0^t v_d(\tau)\mathrm{d}\tau,$$

$$v_d(t) = \begin{cases} 2\ rad/s & \text{if} \quad js_p \leqslant s < (j+1)s_p, \\ 4\ rad/s & \text{if} \quad (j+1)s_p \leqslant s < (j+2)s_p, \end{cases}$$

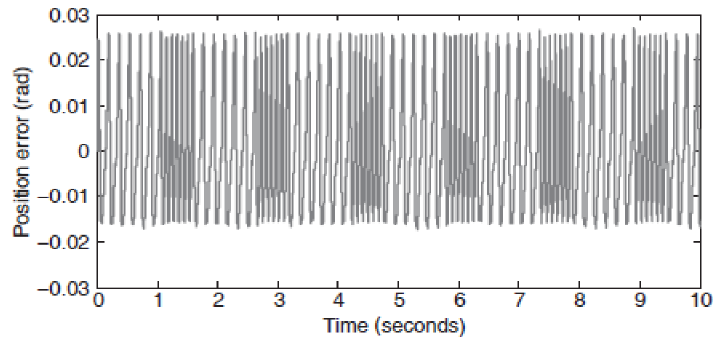


(a) Position

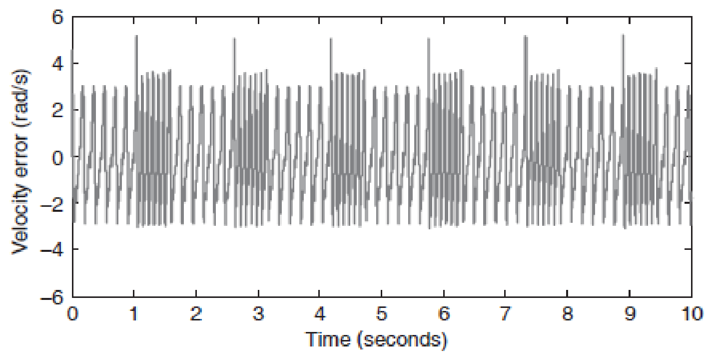


(b) Velocity

Figure: varying reference speed tracking errors without compensation

IO AC position error
IO AC velocity error
IO AC control signal

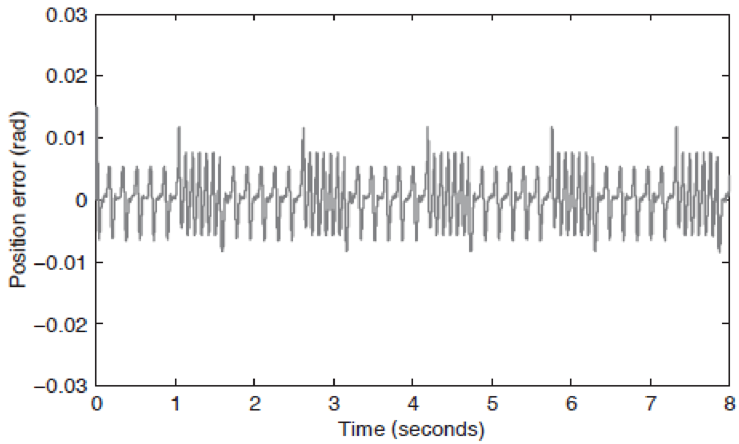


(a) Position

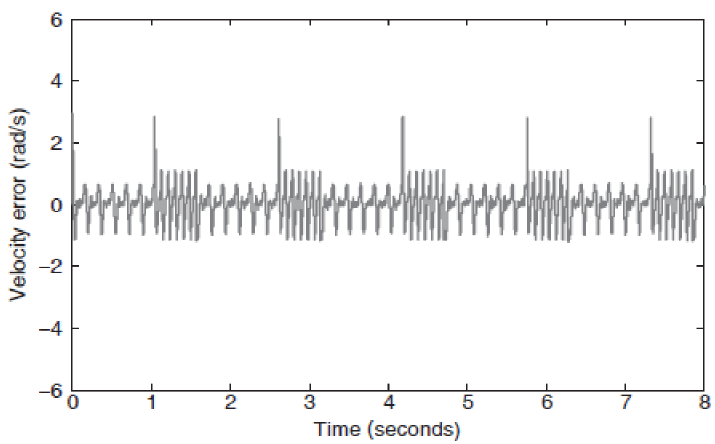


(b) Velocity

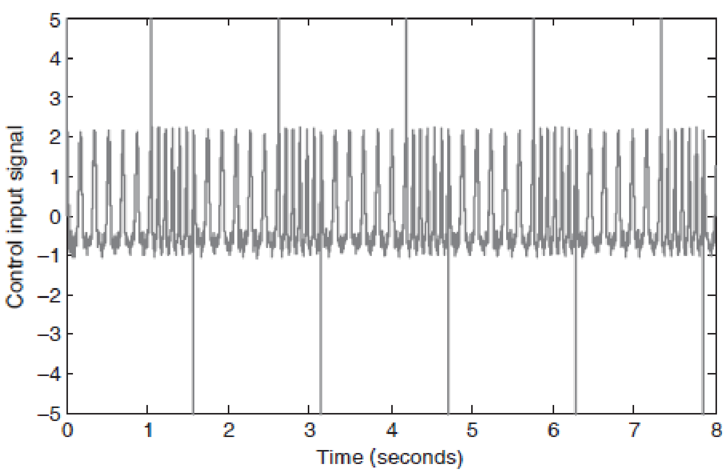


Simulation. Varying reference speed tracking control input signal with

FO AC position error
FO AC velocity error
FO AC control signal

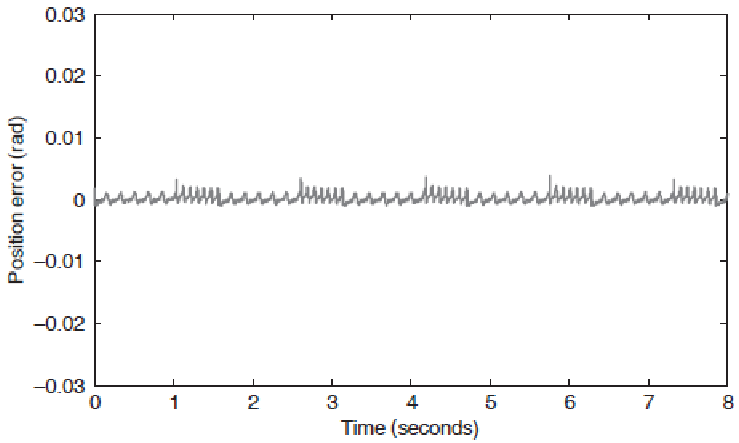

(a) Position

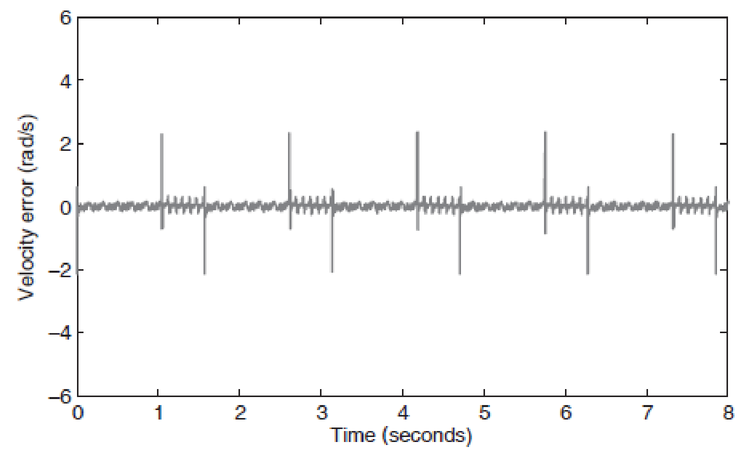

(b) Velocity

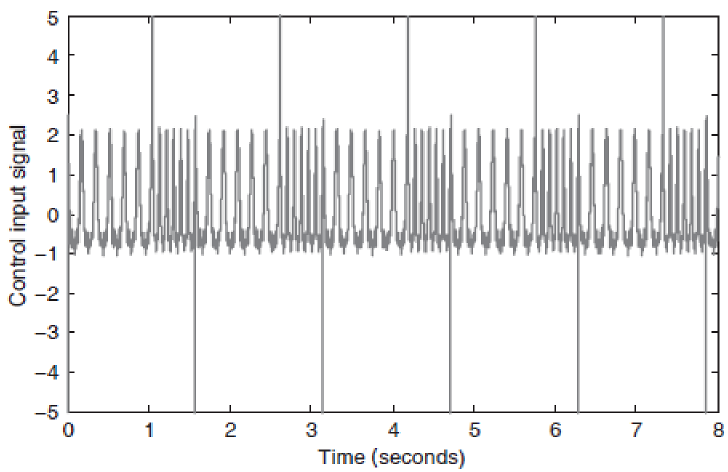

Simulation. Varying reference speed tracking control input signal

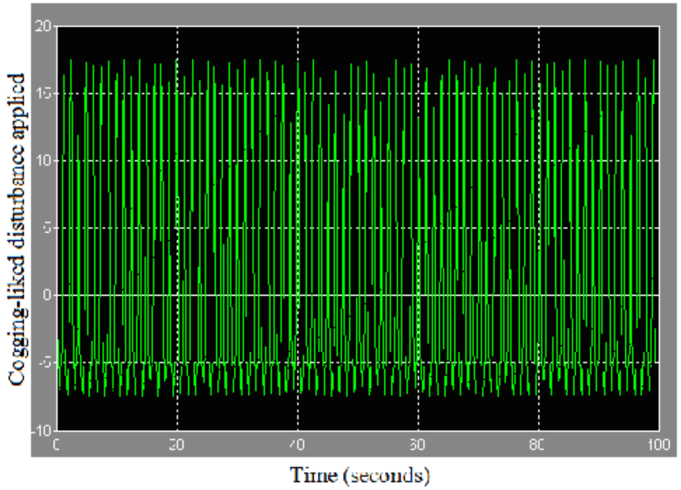


The applied cogging-like disturbance

Constant reference speed tracking errors without compensation

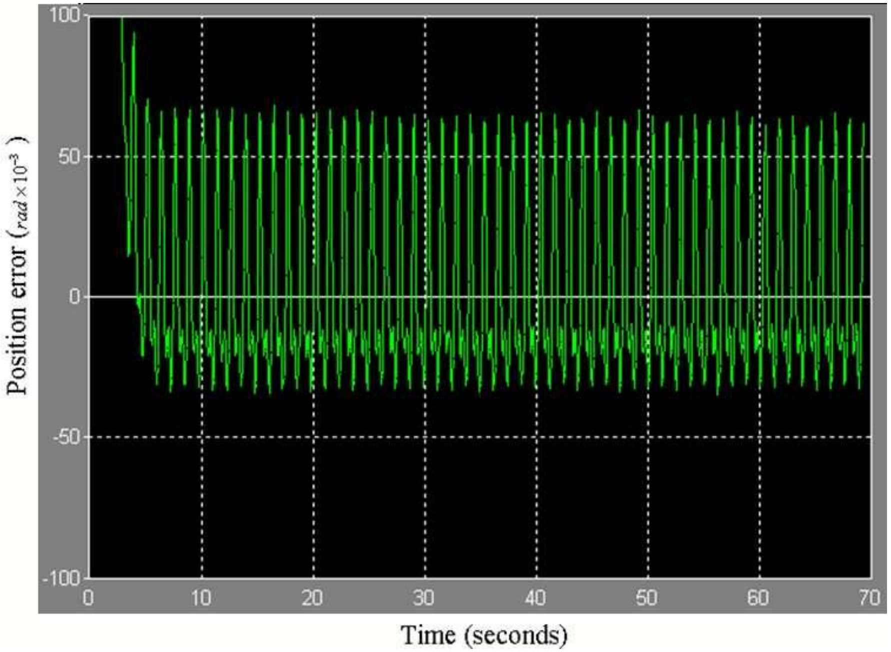


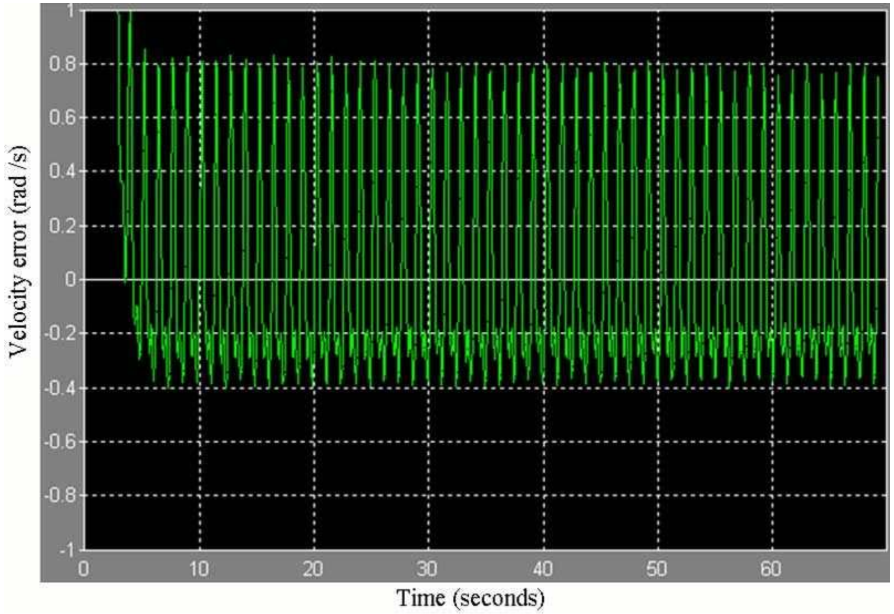

# Experimental validation

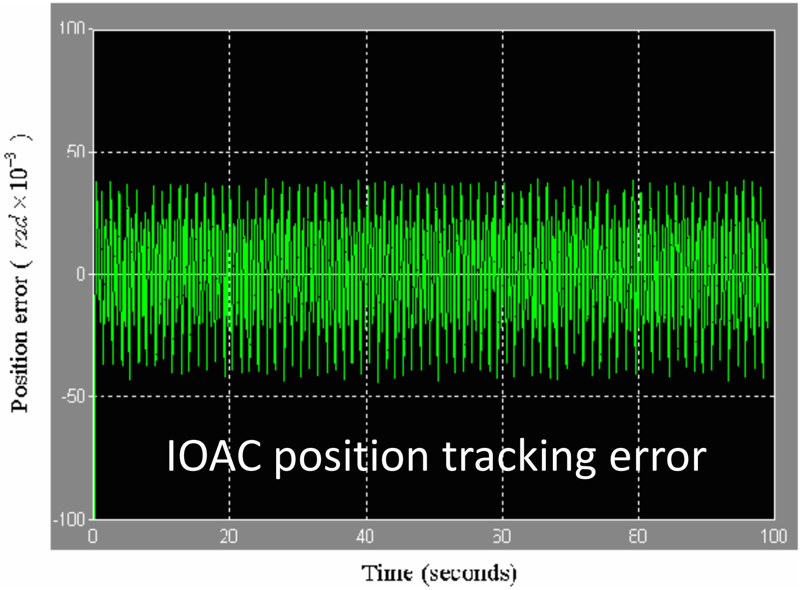


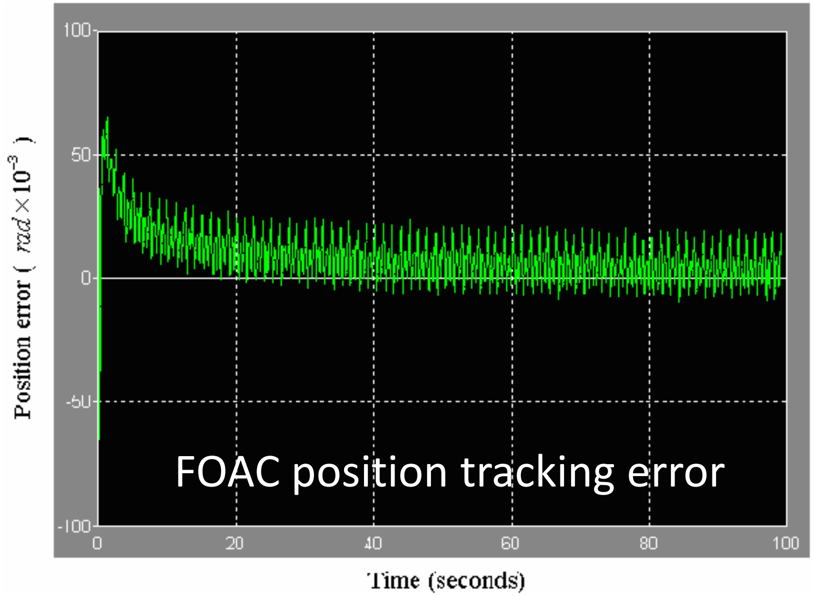


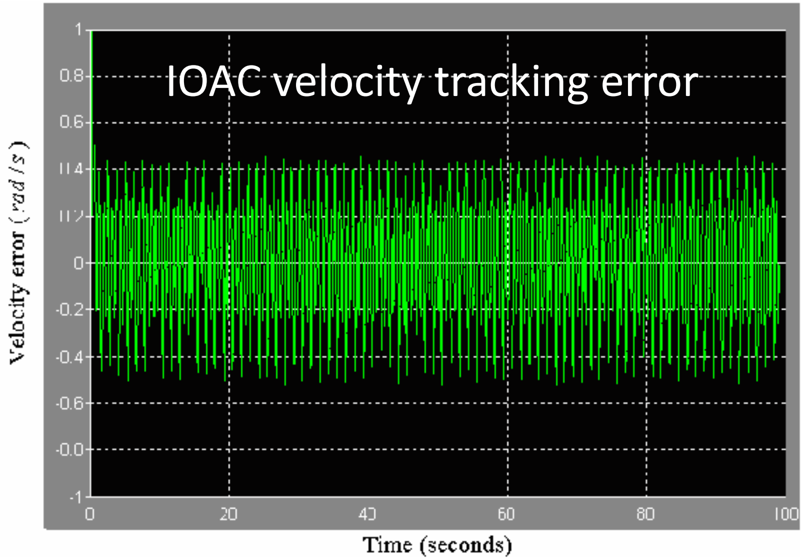


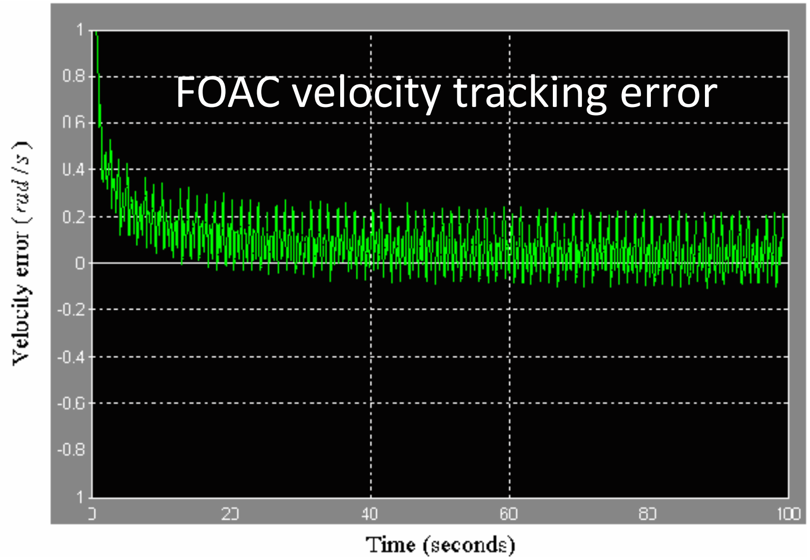

## The state dependent periodic disturbance (SDPD)

Cogging force
Friction force
Etc.

## The general form of SDPD

$$F_{disturnbance} = \sum_{i=1}^{\infty} A_i \, sin(\omega_i x + \varphi_i)$$

## The plant model

$$\dot{\theta}(t) = v(t),$$

$$\dot{v}(t) = u - \frac{a(\theta)}{J} - T_{l'} - B_1 v,$$

$$u = \frac{1}{J}T_m,\ T_{l'} = \frac{1}{J}T_l,\ B_1 = \frac{B}{J},$$

$\theta$: angular position, $v$: velocity; $a(\theta)$ unknown position-dependent cogging disturbance; $J$: moment of inertia; $T_m$: electromagnetic torque; $T_l$: load torque; $B$: viscous friction coefficient

## The adaptive controller

$$u(t) = \dot{v}_d(t) + T_{l'} + \frac{\hat{a}(t)}{J} + \alpha m(t) + \gamma e_v(t),$$

where

$$m(t) := \gamma e_\theta(t) + e_v(t),$$

## The adaptive law in and after the first trajectory period

$$\hat{a}(t) = \begin{cases} z - \mu v, if\ s < s_p & \text{FO AC} \\ \hat{a}_1(t) + \frac{K}{J} m_1(t), if\ s \geq s_p & \text{FO PALC} \end{cases}$$

$${}_0D_t^{\nu} z(t) = \mu[\dot{v}_d(t) + \alpha m(t) + \gamma e_v(t)] + \frac{e_v(t)}{J},$$

$$\begin{cases} v = 1, IO\ AC + PALC \\ v \in (0,1), FO\ AC + PALC \end{cases}$$

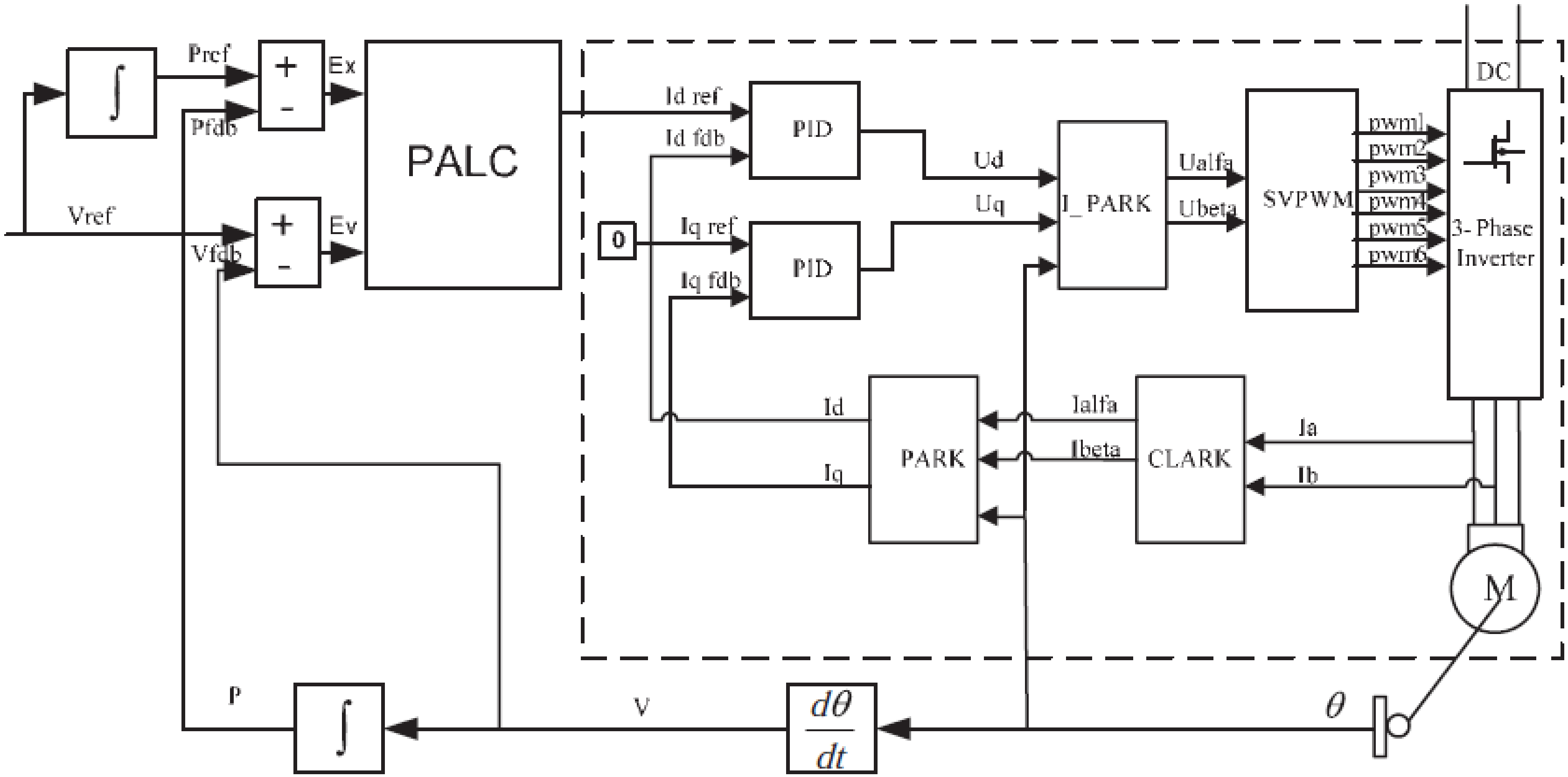


Figure: Block diagram of the cogging PALC in the PMSM position servo system model

Figure: PMSM Specifications

| | | | |
|---|---|---|---|
| Rated power | 1.64 Kw | Rated speed | 2000 rpm |
| Rated torque | 8 Nm | Stator resistance | 2.125 Ω |
| Stator inductance | 11.6 mH | Magnetic flux | 0.387 Wb |
| Number of poles | 6 | Moment of inertia | 0.00289 $kgm^2$ |
| Friction coefficient | 0.0003 Nms | | |

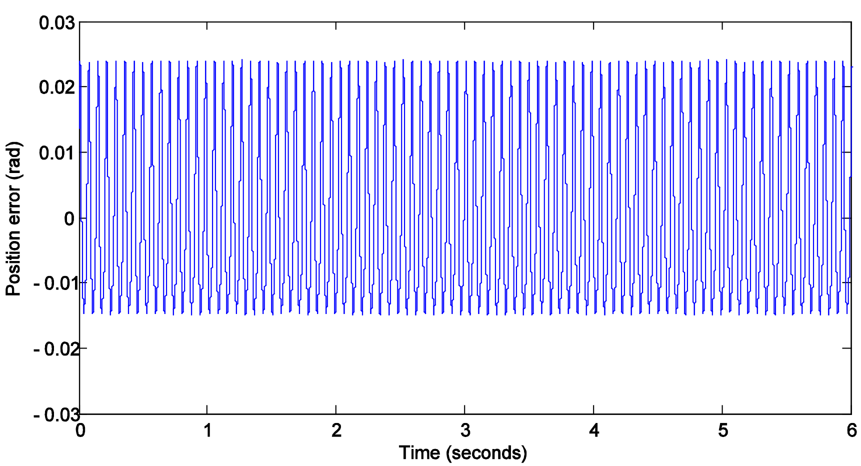


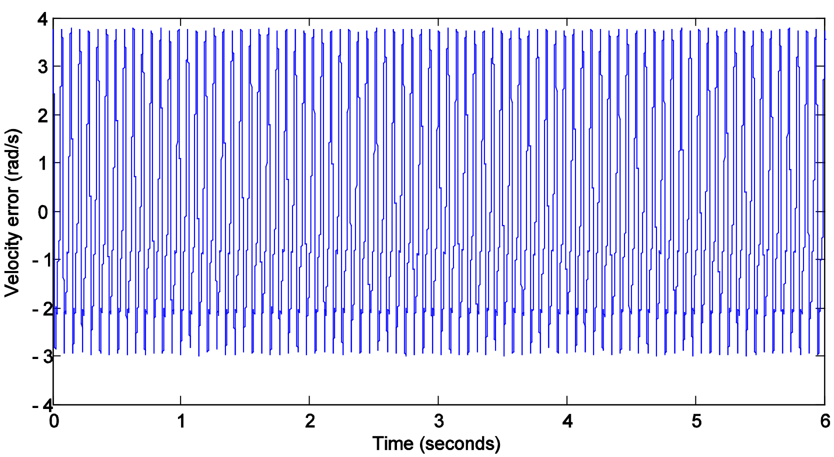


Figure: Tracking errors without any compensation

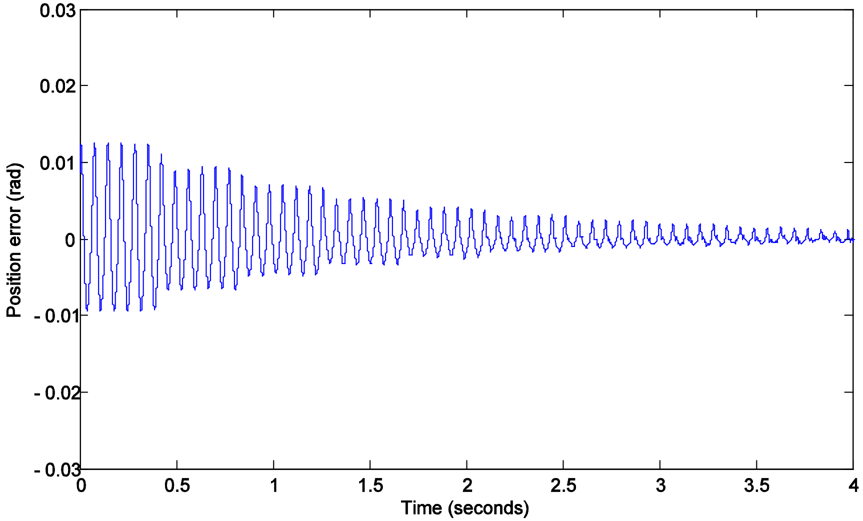


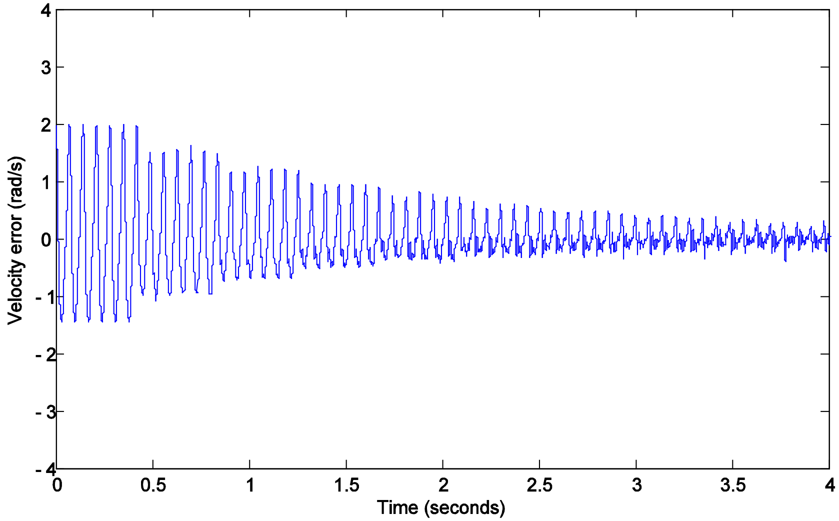


FO AC+PALC (above)
IO AC+PALC (below)

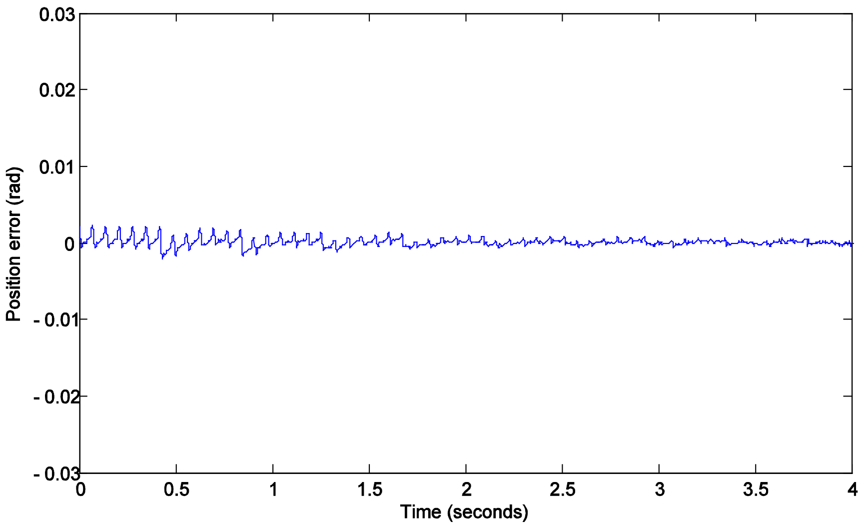


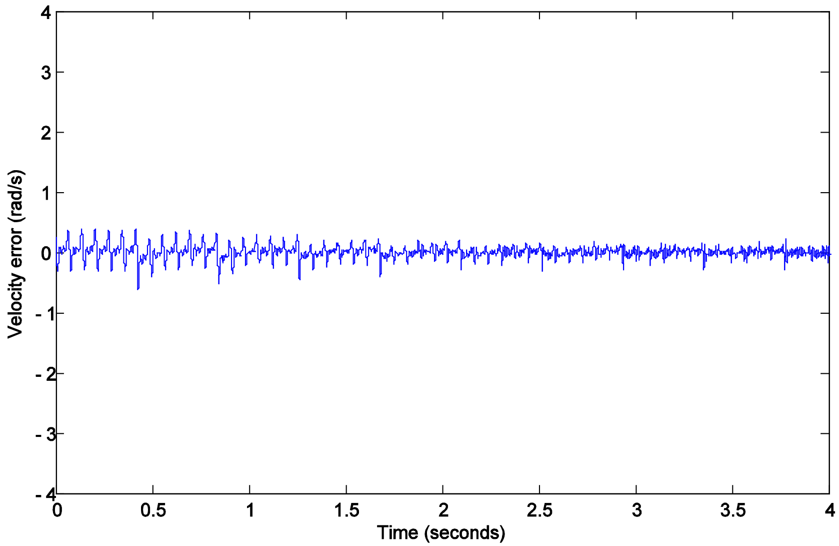

- FO DOB
  - No DOB
  - IO DOB
  - FO DOB
- FO AFC
- FO AC
  - No compensation
  - IO AC
  - FO AC

  For constant ref speed

  - No compensation
  - IO AC
  - FO AC

  For Varying ref speed

- FO AC+PALC
  - No compensation
  - FO AC+PALC
  - IO AC+PALC

# This is the end of session V

# Questions?